Connecting a City by Wireless Backhaul: 3D Spatial Channel Characterization and Modeling Perspectives

Ruonan Zhang, Xiaohong Jiang, Tarik Taleb, Bin Li, Heng Qin, Zhimeng Zhong, and Xiaomei Zhang

The authors explain the methodology and implementation of the spatial channel measurement, and they reveal the urban wireless backhaul channel characteristics which are useful for the design and deployment of wireless backhaul for a smart city.

ABSTRACT

The backhaul forwards aggregated traffic from massive users, machines, and sensors to the core network, and is the key infrastructure to facilitate a smart city. The beamforming and spatial multiplexing technologies enable the wireless multipoint-to-point backhaul to connect dense small cell eNodeBs (eNBs) and macrocell eNBs. Because the spatial characteristics of the backhaul channels, such as the angular power spectra and spreads, determine the interference and capacity performance of the backhaul links, accurate 3D channel modeling is vital for the evaluation and comparison of candidate proposals. In this article, the concepts and methodology of spatial channel modeling are first introduced, and the state-of-the-art models developed by the standardization bodies in recent years are surveyed. Then we present a field measurement campaign on the 3D backhaul channels in an urban street, including the channel sounder implementation, field measurement, multipath parameter estimation, and propagation modeling. The Rx of the sounder (emulating a donor eNB) was installed on the rooftop of a five-story building, and the Tx was located along a street and at different altitudes to emulate a relay eNB. The channel angular power spectra in the elevation and azimuth domains were measured, and the impact by the relay's distance and altitude on the angular spreads was evaluated. In addition, a Laplace model is proposed for the power spectra in both domains. This article not only explains the methodology and implementation of the spatial channel measurement, but also reveals the urban wireless backhaul channel characteristics which are useful for the design and deployment of wireless backhaul for a smart city.

INTRODUCTION

WIRELESS BACKHAUL AND FD-MIMO

Modern cities experienced a dramatic growth in both populations and demand for information service in the last several decades. In the era of Long Term Evolution (LTE), the heterogeneous network (HetNet) has emerged as a flexible and high-capacity architecture. In a HetNet, a macrocell tier is overlaid with a dense tier of small cells (composed of picocells, femtocells, and relays). The small cell eNodeBs (eNBs) provide connectivity to nearby user equipments (UEs), while the macrocell eNBs provide ubiquitous coverage to the others. The former (acting as a relay) forwards the massive traffic from UEs to the latter (acting as a donor), and it is vice versa for the downlink data. Dense deployment of pico/femtocell eNBs with smaller radius can reuse spectrum geographically and also significantly reduce the transmission power. Nowadays, the HetNet has been regarded as the key infrastructure to provide wireless access to not only dense citizens in urban areas but also networked sensors and actuators, which can make city operations more efficient and environmentally safe.

The deployment and popularity of a HetNet require a high-capacity and flexible backhaul infrastructure to connect the relay and donor eNBs. Small cell (relay) eNBs usually need to be quickly deployable, scalable, and cost-effective [1]. Hence, compared to the wired solution (e.g., fiber), the wireless backhaul is a more suitable and viable alternative for the dense urban deployment. The flexibility also allows temporary or mobile deployment (e.g., for sport or entertainment events) and indoor coverage. The emerging large-scale antenna array systems and full-dimensional multiple-input multiple-output (FD-MIMO) technologies [2] are currently under investigation to realize high-performing and cost-effective wireless backhaul. By using a large number of active antenna elements (AAEs) in a planar array, FD-MIMO can form multiple narrow beams and concentrate radiation power in both the azimuth and elevation dimensions. By extending the spatial separation to the elevation domain as well as the azimuth domain, the 3D digital beamforming is attractive to cater for the network densification in cities. As shown in Fig. 1, the donor eNB communicates with multiple relay eNBs simultaneously in a multipoint-to-point manner by space-division multiplexing (SDM). Meanwhile, the radiated power is more concentrated spatially toward the intended receivers, leading to much higher signal strength and less interference to other users.

The current 4G/LTE-Advanced systems operate at 2.6 GHz. Operating backhaul and access links in the same frequency band (in-band wire-

Digital Object Identifier:
10.1109/MCOM.2017.1600234

Ruonan Zhang, Bin Li, and Heng Qin are with Northwestern Polytechnical University; Xiaohong Jiang is with Future University Hakodate; Tarik Taleb is with Aalto University and Sejong University; Zhimeng Zhong and Xiaomei Zhang are with Huawei Technologies Ltd.

0163-6804/17/$25.00 © 2017 IEEE

less backhaul) is preferable for operators. First, the additional cost of buying separate frequency licenses for backhaul is eliminated. Second, the current radio units can be reused to serve the backhaul links. Therefore, the 3D beamforming working in the current frequency band is a promising solution to enable wireless backhaul for a smart city.

3D Channel Characterization for Wireless Backhaul

Capacity and reliability of wireless hackhaul are still challenging issues. In SDM by 3D beamforming, the inter-sector interference is the limiting factor on the link throughput and system capacity. The received signal-to-interference ratio (SIR) depends on the design of AAE arrays and the spatial multipath propagation characteristics (e.g., the distribution and spread of the angular power spectrum). The accurate characterization of the spatial backhaul channels provides the fundamental assumptions for the theoretical analysis and performance simulations of the candidate systems. To describe the multipath propagation in the vertical and horizontal dimensions, a 3D channel model defines the spatial parameters of *azimuth/elevation angle of arrival* (AoA/EoA), *root-mean-square* (RMS) *azimuth/elevation spread of arrival* (ASA/ESA), and the counterparts of these parameters for path departure on the transmitter side. In addition, the angular power spectra in the two domains represent the power arrival distributions over the incident angles, called the *azimuth/elevation power spectrum* (APS/EPS). The angular spreads (ASA, ESA, ASD, and ESD) are the second-order moments of the corresponding power spectra, and indicate the spreads of the power arrival/departure. They have a significant impact on the inter-sector interference in directional beamforming and spatial multiplexing.

Contributions of This Article

The main contributions of this article are twofold. First, we introduce the fundamental concept and methodology for the 3D channel modeling and then survey the current major standardization efforts in recent years. The wireless backhaul channels are essentially different from those between UEs and BSs (as discussed in detail later), but are still less explored.

Second, since the channel characterization and modeling are based on precise field measurements and parametrization, a field measurement campaign on the typical 2.6 GHz in-band backhaul channels is reported. In particular, the design of a MIMO channel sounder developed jointly by Huawei and Northwestern Polytechnical University (NPU) is presented, including the hardware implementation and path parameter estimation method. Then the measurement results of the angular power spectra and spreads in both the elevation and azimuth domains are provided. The Laplace distribution model for APS and EPS is proposed, and the impact of relay eNB's distance and altitude on the angular spreads (ASA and ESA) is revealed based on the measurement data.

The system design of the sounder provides a valuable reference for future spatial channel measurements. The proposed channel models can be used for the deployment and evaluation of the SDM-based wireless backhaul in realistic urban environments.

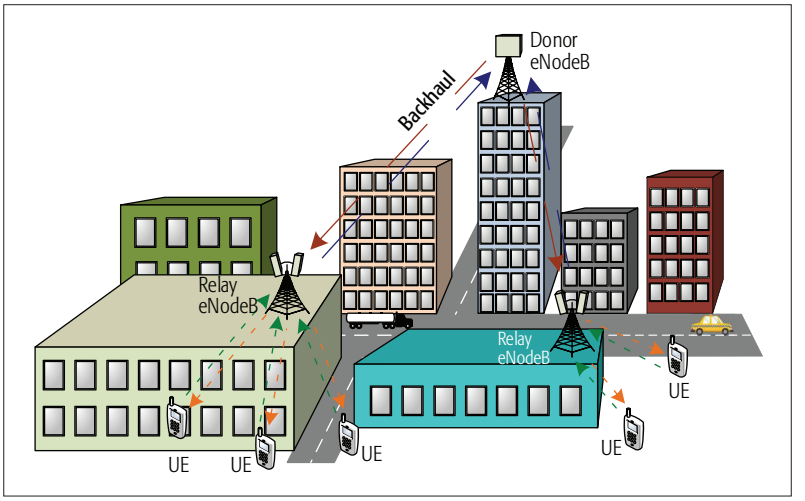

Figure 1. Multipoint-to-point wireless backhaul deployment scenario.

Current 3D Channel Modeling Works

Concept and Methodology of 3D Channel Modeling

The geometry-based stochastic channel models (GSCMs) are ray-based double-directional multipath models for MIMO links. The small-scale (SS) ray parameters (e.g., delay, power, and arrival and departure directions of each propagation path) and the large-scale (LS) channel parameters (e.g., delay spread, angular spread, shadow fading, and cross-polarization ratio) are defined, and their empirical distributions are statistically extracted from field measurements for typical scenarios. GSCMs can generate impulse responses in both the temporal and angular domains, called *channel realizations*, which are then used in wireless system simulations. Channel realizations are the superposition of contributions of rays (plane waves) with three levels of randomness. At first, the LS parameters are drawn stochastically from scenario-dependent distribution functions (by using random number generators and suitable filters). Next, the SS parameters are generated randomly also according to the tabulated distributions and the LS parameters (second moments). Third, by picking (randomly) different initial phases of the scatterers, an unlimited number of different realizations can be generated. The models are usually antenna independent, that is, different antenna configurations and element patterns can be inserted. The GSCMs have become an enabling tool for the link and system-level simulation and performance evaluation of radio interface technologies in realistic propagation conditions.

The traditional GSCMs, such as Third Generation Partnership Project (3GPP) TR25.996-v11 (spatial channel model, SCM) [3] and WINNER I [4], are 2D in the sense that only the azimuth-related parameters (i.e., AoA/AoD and ASA/ASD) are characterized, and the elevation angles of propagation paths are neglected. Inspired by the attractive features and potential benefit of FD-MIMO and 3D beamforming, several standardization projects in recent years, such as WINNER,

The system design of the sounder provides a valuable reference for future spatial channel measurements. The proposed channel models can be used for the deployment and evaluation of the SDM based wireless backhaul in realistic urban environments.

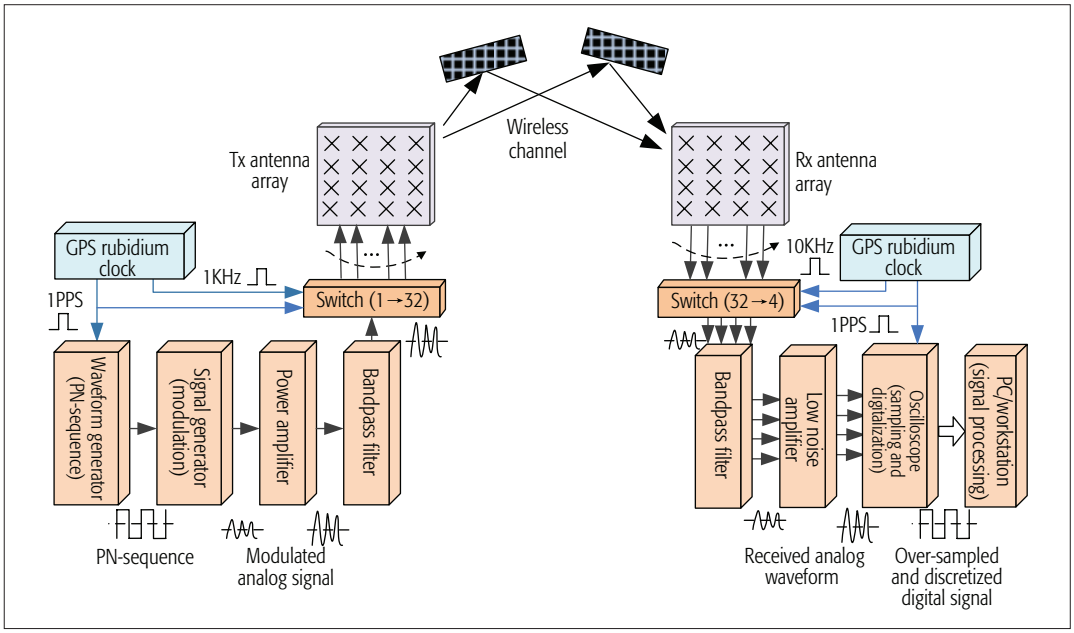

Figure 2. The architecture of the MIMO channel sounder.

3GPP, COST2100, and METIS, have made significant achievements in defining the 3D bidirectional, dual-polarized MIMO channel models. True elevation angles are associated with signal paths. The new SS parameters EoA/EoD and two new LS parameters ESA/ESD are defined in the extended models. Their distributions and correlations with other LS fading parameters such as the path loss and delay spread are also given for specific scenarios.

Current 3D Channel Models

The major efforts in the 3D channel modeling by the standardization bodies are briefly introduced as follows.

The WINNER family is a set of GSCMs, describing various environments including outdoor, indoor, and outdoor-to-indoor. The models are parameterized using results from an extensive set of measurement campaigns. The 3D channel model, WINNER+ [5], has been evolved from the earlier phases of WINNER I and II (SCM wideband extension, SCME). The novel features include the elevation parametrization, scenario-dependent polarization modeling, new scenarios, and so on. The generalization from 2 to 3D uses the same modeling approach in generating the elevation-related parameters. The composite APSs of all clusters are modeled by the wrapped Gaussian distribution. The AoAs of paths are generated by applying the inverse Gaussian function with input parameters of cluster power and ASA given for specific scenarios. The cluster EPSs have the Laplace distribution. Then the elevation angles of paths are determined by the same procedure with the original ASA values replaced by ESAs. Due to the limit of available measurement results, the cross-correlation coefficients of the new LS parameters are set as zero if the measured values are less than 0.4. Furthermore, if the measurement data for a scenario are not available, it is proposed to borrow values for other scenarios.

3GPP has also paved the way to full 3D channel models. 3GPP established a study item in 2012 [6] on 3D channel modeling. The findings are captured in the latest technical report (TR36.873) released in June 2015 [7]. The new scenarios for the UE-specific elevation beamforming, such as the UMa with high outdoor/indoor UE density, are specified. The modeling of the elevation-domain parameters is similar to that in WINNER.

European Cooperation in the Field of Scientific and Technical Research (COST) Actions in the field of wireless communications started from Action 207 (Digital Land Mobile Communications), followed by a series of successful Actions of COST 231, 259, 273, and, finally, 2100 [8]. The channel model in COST2100 characterizes the 3D channel at the individual cluster level. A cluster (scattering object) is not specific to one single link but depicted as an ellipsoid in space. The cluster angular spread (CAS) includes the arrival/departure power spread in both the azimuth and elevation planes. It is proposed that the CAS follows the lognormal distribution with a base of 10.

Another important effort is from the Mobile and Wireless Communications Enablers for the Twenty-twenty Information Society (METIS) project [9]. METIS has the goal to provide solutions for the new challenges in the fifth generation (5G) systems. Based on extensive measurement campaigns in the propagation scenarios relevant to 5G and at various frequencies between 2 and 60 GHz, new channel models are proposed for accurate 3D propagation characterization, massive MIMO with high spatial resolution, and dual-mobility links (e.g., vehicle-to-vehicle communications) [10]. The modeling approaches include the GSCM, a map-based site-specific deterministic model (based on ray-tracing), and a hybrid model for scalability. In the GSCM approach, the generation of arrival and departure directions in the azimuth and elevation domains follows the distribution models in 3GPP TR14-36873 [7] discussed above.

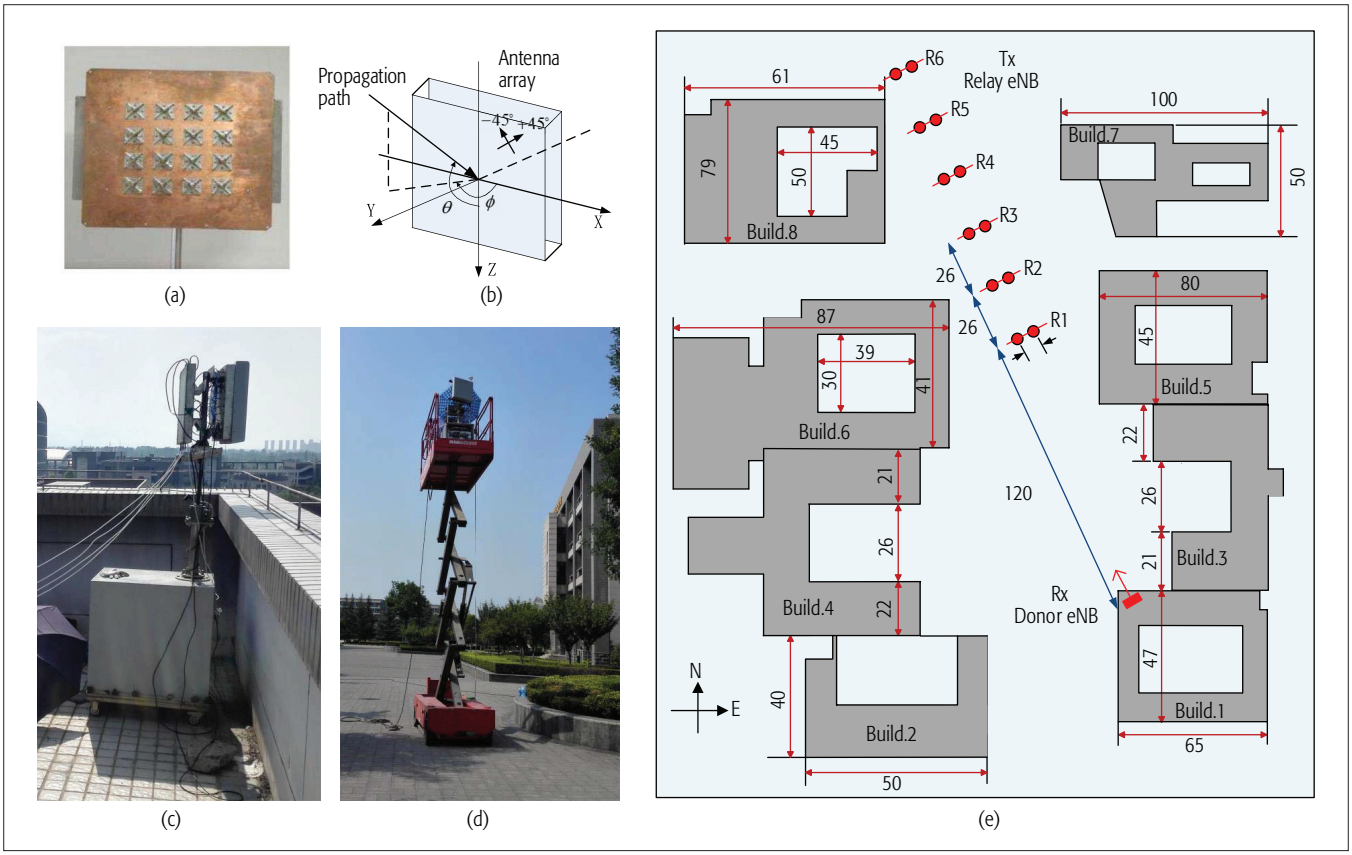

Figure 3. The channel sounder setting and measurement positions: a) antenna array; b) coordinate; c) receiver (donor eNB); d) transmitter (relay eNB); e) measurement positions (distance unit: meter).

Modeling for Wireless Backhaul Channels

The existing 3D channel models developed in recent years mainly focus on the cellular communication links between fixed BSs and mobile UEs [11]. However, the backhaul scenario, which has been less explored, is essentially different, in particular in the following three aspects:

- Relay eNBs are above the height of pedestrians. They are usually mounted on lampposts or exterior walls of buildings. The altitude will have a significant impact on the channel characteristics.
- The relay eNBs employ directional antennas (or antenna arrays) instead of omnidirectional antennas used in UEs. The main lobe of a relay eNB is pointing to its target donor eNB to concentrate radiated power. Since there are no paths emitting from the back of the directional antenna, the angular power spectra on both the relay and donor eNBs may change.
- The eNBs are fixed, and thus there is no Doppler effect. Therefore, the channel modeling focuses on the spatial properties. The high-performing wireless backhaul techniques set new requirements for radio channel and propagation modeling, which has motivated this work.

Measurement System and Scenario

Measurement System

The measurement campaign on the wireless backhaul channels was conducted using a MIMO radio sounder. Its architecture is illustrated in Fig. 2, and photographs of the transceivers are presented in Figs. 3c and 3d. The sounder probes channels in the time domain based on the direct sequence spread spectrum (DSSS) approach. The carrier of 2.6 GHz frequency is modulated by cyclic pseudo-noise (PN)-sequences and transmitted over the air. The length of a PN-sequence is 1023 chips and the rate is 62.5 Mchips/s.

The Tx and Rx are both equipped with a dual-polarized uniformed planar array (UPA). One UPA is composed of 16 pairs of cross-patches organized in a 4 × 4 matrix with spacing of half a wavelength (Fig. 3a). Each pair includes two dipoles in ± 45° polarizations, and hence there is a 4 × 4 dipole array in either polarization. A dipole has 7 dBi peak gain and a half-power beamwidth of –70° to +70° in both the azimuth and elevation dimensions. The incident angle of an impinging wave is defined with respect to the coordinate in Fig. 3b. The spatial and polarization domains are covered by measuring the channel responses between multiple transmitting and receiving antenna pairs sequentially in a time-division multiplexing (TDM) manner. On the Tx side, the signal source is connected to the UPA with a microwave switch with 1 input and 32 output ports. The 32 dipoles are stimulated one by one through the switch, and each dipole transmits 10 frames for 1 ms to probe the channel. Each frame contains five PN-sequences plus header and tail, and lasts for 0.1 ms. On the Rx side, a microwave switch with 32 input and 4 output ports is connected to the UPA, which selects 4 co-polarized dipoles in one column and outputs the received signals. The radio signals are then processed by low noise amplifiers (LNAs) and bandpass filters,

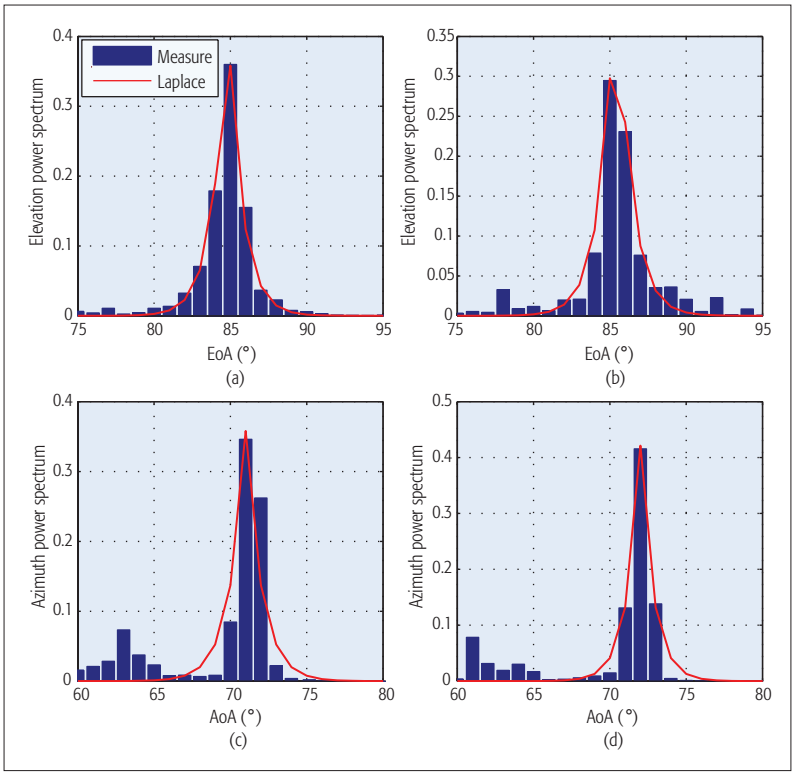

Figure 4. The measured angular spectra (EPS and APS) at different relay-to-donor distances and relay altitudes: a) region = 1, altitude = 4.5 m; b) region = 3, altitude = 7 m; c) region = 1, altitude = 4.5 m; d) region = 2, altitude = 7 m.

and finally input into the 4 ports of a Tex70608 oscilloscope where they are sampled by the rate of 625 MHz and stored for offline processing. The microwave switch connects 4 dipoles in one column for 0.1 ms to receive one complete frame and then switch to the next column. Thus, within the transmitting time of one Tx dipole (1 ms), the 8 columns of the Rx UPA take 8 × 0.1 = 0.8 ms for reception, while all 32 dipoles receive a complete frame of the sounding signal. The antenna elements are switched almost instantaneously so that the channel response remains practically constant within the Rx antenna switching period. The waveforms captured on the 4 × 4 rectangular array in one polarization during this period is a *spatial channel snapshot*, which is then used to estimate the power and 2D angle of arrival of the propagation paths. To ensure signal timing and antenna switching synchronization, two GPS-triggered rubidium clocks are used at the transceivers to provide reference clocks of 1 Hz, 1 kHz, and 10 kHz pulses per second (PPS).

The path parameters are extracted using super-resolution techniques including two tasks. First, paths are resolved from the captured radio waveforms jointly by sliding correlation (between the received signals and the spreading code) in the time domain and spatial smoothing in the space domain. Second, based on the array complex impulse responses received on the UPA, the 2D incident angles of the paths are estimated using the subspace-decomposition algorithm. Readers are referred to [12] for detailed presentation of the parameter estimation algorithm. System calibration is performed on each measurement day to compensate the transfer functions of the radio chains of the Rx in the captured channel impulse responses. The 3D radiation pattern of the Rx UPA (steering vectors) has been measured in an anechoic chamber and is incorporated in the angle of arrival estimation algorithm to remove the antenna effect. Thus, the antenna-independent channel characteristics are obtained.

Measurement Scenario

The measurement campaign was conducted on the campus of NPU. One important deployment scenario of small cells is along urban streets to forward high traffic load generated from pedestrians and passengers on vehicles. We consider the multipoint-to-point scenario where a donor eNB connects multiple relay eNBs by SDM, as shown in Fig. 1. The wireless backhaul channels in such a street canyon environment with line of sight (LOS) were measured in this campaign. Since multiple beams would be formed on the donor eNB antenna array in this scenario, we focused on the power arrival profile at the donor eNB. Furthermore, according to the channel reciprocity, the power departure profiles were also obtained by swapping the directions of the incoming paths.

The Rx was installed on the rooftop of a five-story office building by the roadside as the donor eNB (Fig. 3c). Its antenna panel was 24.5 m high and above the other buildings in the surrounding environment. The Tx was placed in six regions along the street, where the distances to the Rx changed from 120 to 250 m horizontally, as illustrated in the map in Fig. 3e. The regions were evenly spaced by 26 m. In each region, the Tx was placed at two positions which were parallel and spaced by 2 m. Furthermore, to emulate a relay eNB, the Tx was raised up to three altitudes (2, 4.5, and 7 m) by an elevator at each position (Fig. 3d). Thus, the impact of the relay distance, altitude, and scattering environment on the wireless backhaul channel could be studied.

In this work, the signals when both transceiver antennas were +45° polarized (with respect to the Rx coordinate system) were used and the co-polarization measurements were performed. At each relay position and altitude, the 32 dipoles on the Tx UPA transmitted for 25 cycles. Thus, the channel was sounded by 32/2 × 25 = 400 times in one polarization, and 400 independent channel snapshots were captured (as mentioned earlier, one snapshot was the array signal received by the Rx UPA during 0.8 ms when one Tx dipole was transmitting). Furthermore, from 2 measured positions in one region, 400 × 2 = 800 snapshots were obtained for a given relay-donor distance and altitude. From the array signal of each snapshot, the 10 most significant multipath components (MPCs) were resolved from the waveforms and parameterized. Based on the EoA, AoA, and power of these MPCs, the angular power spectra and spreads were obtained.

There was variation among the 800 snapshots at one altitude in a region, caused by the movements of the Tx over a small distance and the people and vehicles in the scattering environment. However, the relay-donor distance, altitude, and surrounding buildings remained stationary. Therefore, the variation among the snapshots is

referred to as the *small-scale spatial fading*. The statistics of the snapshots collected from one Tx region and altitude represent the small-scale fading of the channel. On the other hand, the variation of the model parameters (e.g., mean and variance) among different relay regions and altitudes reflects the *large-scale spatial fading*.

Measurement Results and Modeling

Angular Power Spectrum and Spread in the Elevation Domain

For a given relay-donor distance and relay's altitude, the EPS and ESA are calculated from the power and EoAs of the 800 × 10 = 8000 sample MPCs (800 channel snapshots and 10 MPC samples per snapshot). As illustrative examples, the obtained EPSs when the Tx was placed 4.5 m high in region 1 and 7 m high in region 3 are plotted in Figs. 4a and 4b, respectively.

As shown in Fig. 4, the power arrival mostly concentrates in the main clusters in this LOS scenario. Hence the statistical model for the EPS of the main cluster is established. Since the main clusters are symmetric with one peak, we consider the candidate distribution functions of *Laplace*, *normal*, and *Cauchy* probability distribution functions (PDFs). By using the AIC-testing method, they are compared in fitting the empirical power spectra, and the Laplace distribution can model the measurement graphs best. The Laplace PDF is denoted by $Lap(\mu_E, b_E)$, where μ_E and b_E are the location parameter and the scale parameter, respectively. For example, the best-fit Laplace PDFs, obtained with minimum mean square error (MMSE), are superimposed in Figs. 4a and 4b. The location parameter μ_E is approximated by the LOS direction, that is, $\mu_E = \theta_{LOS}$ where θ_{LOS} is the EoA of the LOS path and calculated geometrically according to the geographic locations of the relay and donor eNBs.

The scale parameter b_E describes the spread of the main cluster, and $\sqrt{2}b_E$ (the second moment of the Laplace distribution function) is actually the ESA of the main cluster. The values of b_E for all the measurement regions and altitudes are plotted in Fig. 5. First, it is observed that the impact of the relay altitude, denoted by h_{rel}, is remarkable. For a given relay-donor distance (denoted by d_{rel}), b_E is larger when the relay altitude is increased. This shows that higher relay altitude leads to larger ESA at the donor eNB. Second, as d_{rel} increases, b_E has fluctuations, and the linear regressions on the measured values show two tendencies. When the relay is low (2 m high), the expectation of b_E is almost constant for various d_{rel}. But b_E has a common decreasing tendency at the altitudes of 4.5 and 7 m. This indicates that when the relay is moved away from the donor, the channel ESA almost does not change if the relay is close to the ground, but decreases if the relay is placed higher. Third, it can be seen that when the distance is increased, the values of b_E at the three altitudes converge. Therefore, the impact of a relay's altitude is more significant when it is close to the donor horizontally, and vice versa.

Figure 5 shows that b_E varies linearly with respect to the relay-donor distance, and the slope and intersect depend on the relay altitude. Therefore, b_E can be modeled by a linear function with respect to the independent variable d_{rel} and the parameter h_{rel}, expressed as

$$b_E = \alpha(h_{rel})d_{rel} + \beta(h_{rel}). \quad (1)$$

The coefficients of the linear function for the three measured relay altitudes, h_{rel} = 2, 4.5, and 7 m, are obtained directly by the linear regression as plotted in Fig. 5. The results are (α, β) = (0, 0.33), (−0.004, 1.457), and (−0.002, 1,274). The coefficients for other h_{rel} from 2 to 7 m can be derived by interpolation. The linear model in Eq. 1 reflects the impact of the relay's altitude and horizontal distance and their interaction on the channel ESA. Based on the linear model, the value of b_E for the continuous relay distance (in the range of $d_{rel} \in$ [120, 250] m) and altitude (in the range of $h_{rel} \in$ [2, 7] m) can be determined. Then the realizations of the main cluster EPS can be generated by the Laplace model of $Lap(\theta_{LOS}, b_E)$.

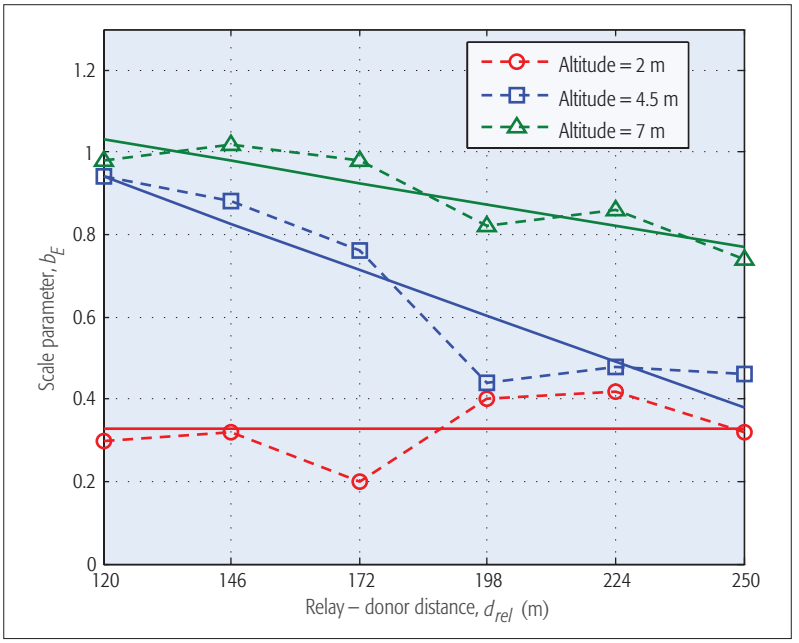

Figure 5. The scale parameter b_E of the best-fit Laplace distribution functions for the measured main cluster EPS.

Angular Power Spectrum and Spread in the Azimuth Domain

Following the same approach for the elevation domain, the measured APSs when the Tx was located at 4.5 m in region 1 and 7 m in region 2 are plotted in Figs. 4c and 4d for demonstration. In addition to the main clusters, due to the scattering and reflection by the roadside buildings, small clusters can be observed. Again, the symmetric shape of the main clusters suggests the candidate functions of *Laplace*, *Normal*, and *Cauchy* PDFs. The AIC-testing indicates that the APSs of the main clusters can be best fit by the Laplace distribution, which is denoted by $Lap(\mu_A, b_A)$. $\sqrt{2}b_A$ is the ASA of the main cluster.

The location parameter μ_A is the AoA of the LOS direction, denoted by ϕ_{AoA} and calculated geometrically. The scale parameter b_A of the best-fit Laplace PDFs is shown in Fig. 6a for the relay distances and altitudes measured in this campaign. As can be observed, as the horizontal distance d_{rel}

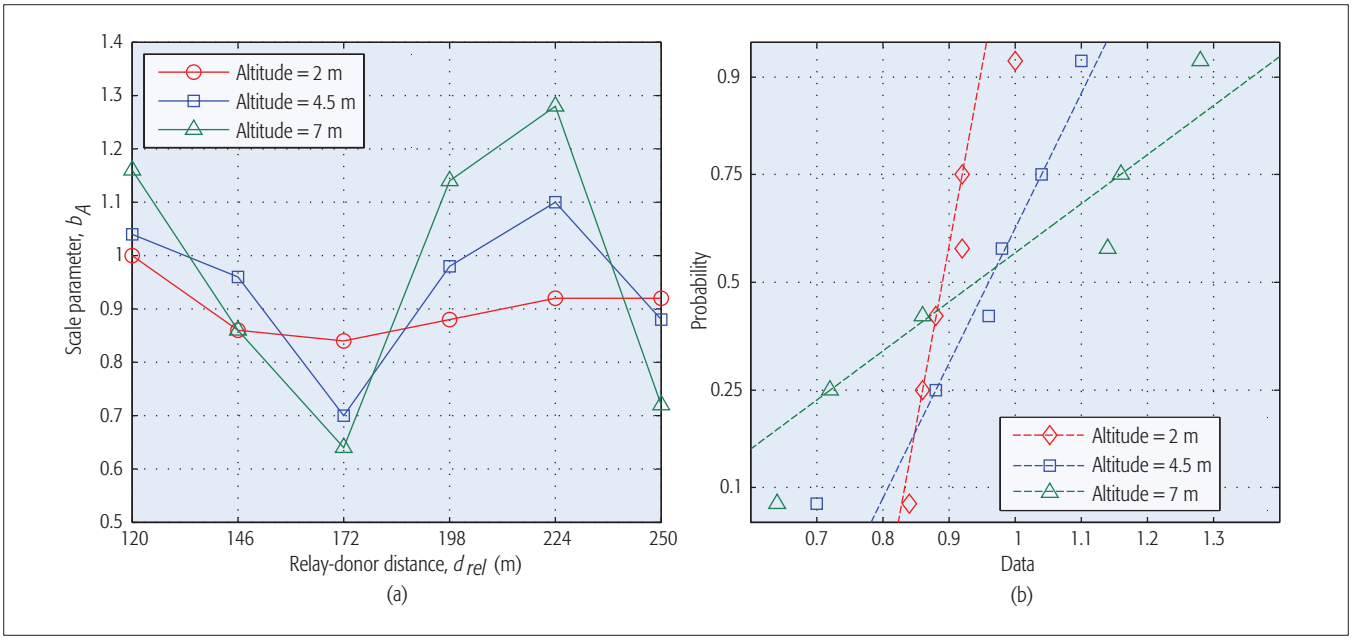

Figure 6. The scale parameter b_A of the best-fit Laplace distribution functions for the measured main cluster APSs: a) measurement results of b_A; b) probability plot of b_A.

increases, b_A presents considerable fluctuations at all the altitudes. From the street map in Fig. 3e, the building layout by the roadsides is irregular. There are gardens of grass and small trees between the buildings, and the distance between the Tx and roadside buildings varies. This indicates that the change of the roadside building layout has a significant impact on the ASA of the backhaul channel. Furthermore, interesting properties of b_A can be found. First, the variation tendencies at the three altitudes are coincident with each other, as plotted in Fig. 6a. Therefore, the impact of surrounding environment is consistent for different relay altitudes. Second, when h_{rel} is larger, the fluctuation of b_A is more significant. This indicates the interaction between h_{rel} and d_{rel}. Higher relay altitude leads to larger variance of b_A when the relay is located at different distances.

To model the distribution of b_A, the probability plots in Fig. 6b testify to the measurement values against the normal distribution using the function *normplot* in MATLAB. As observed, the sample values are close to the lines and hence follow the normal distributions well. In addition, the Kolmogorov-Smirnov test has shown that the measurement results of b_A have the normal distribution at the significance level of 0.05. Therefore, we propose the normal distribution model for b_A of the main cluster APS, that is, $b_A \sim N(\mu_b, \sigma_b^2)$, where μ_b and σ_b are the mean and standard deviation (STD), respectively. According to the fitting results plotted in Fig. 6b, μ_b of the normal PDFs for the three relay altitudes are 0.90°, 0.94°, and 0.97°. Hence, we can approximate μ_b by a constant, that is, $\mu_b \approx 0.94°$. The values of σ_b of the normal PDFs are 0.05°, 0.15°, and 0.26° which increase quite linearly for the relay altitudes. Therefore, we can model σ_b by a linear function with respect to h_{rel}. By using the linear regression, it can be derived as $\sigma_b = 0.042\, h_{rel} - 0.036$. The value of σ_b for the relay altitude between 2 and 7 m can be calculated simply by the linear function.

To generate channel realizations, μ_b and σ_b are first determined according to d_{rel} and h_{rel} as specified above. Then the scale parameter b_A is drawn stochastically by the normal distribution $N(\mu_b, \sigma_b^2)$. Finally, the main cluster APS is obtained as the Laplace distribution of $Lap(\phi_{AoA}, b_A)$.

Conclusion

High-capacity and scalable wireless backhaul will be essential for the HetNet in providing ubiquitous coverage for dense citizens and sensors in smart cities. The successful deployment of wireless backhaul using high-throughput spatial multiplexing requires a solid understanding and accurate propagation models of the radio channels between relay and donor stations. In this article, we have surveyed the development of 3D channel models defined by the standardization bodies in recent years. The principles, methodologies, and channel sounder implementation for 3D channel modeling are introduced. Then a field channel measurement campaign on the 3D co-polarized wireless backhaul channels in a typical urban street environment is presented. We have shown that the APS and EPS of the main MPC cluster can be well modeled by the Laplace distribution. The location and scale parameters have been formulated with respect to the relay altitude and distance. The measurement results provide an initial insight into the 3D multipath propagation of street backhaul channels and how the relay altitude and distance affect the channel characteristics. Furthermore, the Laplace model and stochastically generated channel realizations can be used for the analysis and simulations of the wireless backhaul technologies, such as the SIR evaluation and interference cancellation in beamforming and spatial multiplexing. Third, the proposed power spectrum model can extend current 3D GSCMs reviewed previously.

The street backhaul channel model can be further extended to the packet level. By considering the wireless channel dynamics, the packet-level model describes the link SIR or packet error rate

on the basis of packet transactions [11, 13]. It will be a useful tool for fast simulations of upper-layer protocols and applications of the SDM wireless backhaul. Another avenue of interest is the channel characterization for the millimeter-wave (mmWave) capabilities at frequencies such as 28 and 38 GHz. The mmWave communications are expected to provide multi-gigabit rates to further enhance the backhaul capacity.

Acknowledgment

This work was partly supported by NSFC (61571370 and 61601365), Natural Science Basic Research Plan in Shaanxi Province (2015JM6349 and 2016JQ6017), and National Civil Aircraft Major Project of China (MIZ-2015-F-009)).

References

[1] "Macrocell Mobile Backhaul Equipment and Services Market Share and Forecast Report," *Infonetics Research*, tech. rep., 2012.
[2] Y.-H. Nam *et al.*, "Full-Dimension MIMO (FD-MIMO) for Next Generation Cellular Technology," *IEEE Commun. Mag.*, vol. 51, no. 6, June 2013, pp. 172–79.
[3] 3GPP Tech. Spec. Group Radio Access Networks, "Spatial Channel Model for Multiple Input Multiple Output (MIMO) Simulations (Release 11)," tech. rep. TR 25.996 v11.0.0, Sept. 2012.
[4] "D5.4: Final Report on Link and System Level Channel Models," WINNER, tech. rep., Oct. 2005.
[5] "D5.3: WINNER+ Final Channel Models," WINNER, tech. rep. v. 1.0, June 2010.
[6] "Study on 3D-Channel Model for Elevation Beamforming and FD-MIMO Studies for LTE," 3GPP TSG RAN Plenary, Barcelona, Spain, Study Item Description RP-122034, Dec. 2012.
[7] 3GPP Tech. Spec. Group Radio Access Networks, "Study on 3D Channel Model for LTE (Release 12)," tech. rep. TR 36.873 v. 12.2.0, June 2015.
[8] R. Verdone and A. Zanella, Eds., *Pervasive Mobile and Ambient Wireless Communications COST Action 2100*, Springer, 2012.
[9] A. Osseiran *et al.*, "Scenarios for 5G Mobile and Wireless Communications: The Vision of the METIS Project," *IEEE Commun. Mag.*, vol. 52, no. 5, May 2014, pp. 26–35.
[10] "METIS Channel Models," tech. rep. ICT-317669, July 2015.
[11] R. Zhang *et al.*, "Channel Measurement and Packet-Level Modeling for V2I Spatial Multiplexing Uplinks Using Massive MIMO," *IEEE Trans. Vehic. Tech.*, vol. 65, no. 10, Oct. 2016, pp. 7831–43.
[12] R. Zhang *et al.*, "Two-Dimensional DoA Estimation for Multipath Propagation Characterization Using the Array Response of PN-Sequences," *IEEE Trans. Wireless Commun.*, vol. 15, no. 1, Jan. 2016, pp. 341–56.
[13] R. Zhang and L. Cai, "A Packet-Level Model for UWB Channel with People Shadowing Process Based on Angular Spectrum Analysis," *IEEE Trans. Wireless Commun.*, vol. 8, no. 8, Aug. 2009, pp. 4048–55.

Biographies

Ruonan Zhang [S'09, M'10] received his B.S. and M.Sc. degrees from Xi'an Jiaotong University, China, in 2000 and 2003, respectively, and his Ph.D. degree from the University of Victoria, Canada, in 2010, all in electrical and electronics engineering. He worked as an IC architecture engineer at Motorola Inc. and Freescale Semiconductor Inc. in Tianjin, China, from 2003 to 2006. Since 2010, he has been with the Department of Communications Engineering at Northwestern Polytechnical University, Xi'an, Shaanxi, China, and he is currently a professor. His current research interests include wireless channel measurement and modeling, architecture and protocol design of wireless networks, and satellite communications. He has been a recipient of the New Century Excellent Talent Grant from the Ministry of Education of China, and the best paper award of IEEE NaNA 2016. He has served as a Local Arrangement Co-Chair for IEEE ICCC 2013, and an Associate Editor for the *Journal of Communications and Networks*.

Xiaohong Jiang [SM] is currently a full professor of Future University Hakodate, Japan. Before joining Future University, he was an associate professor, Tohoku University, from February 2005 to March 2010. His research interests include computer communications networks, mainly wireless networks and optical networks, network security, interconnection networks for massive parallel computing systems, routers/switches design for high performance networks, and so on. He has published over 280 technical papers in premium international journals and conferences, which include over 60 papers published in top IEEE journals and top IEEE conferences, like *IEEE/ACM Transactions on Networking*, the *IEEE Journal of Selected Areas on Communications*, *IEEE Transactions on Parallel and Distributed Systems*, *IEEE Transactions on Communications*, and IEEE INFOCOM. He was the winner of the Best Paper Award and Outstanding Paper Award of IEEE HPCC 2014, IEEE WCNC 2012, IEEE WCNC 2008, IEEE ICC 2005 Optical Networking Symposium, and IEEE/IEICE HPSR 2002. He is a member of ACM and IEICE.

Tarik Taleb [M] (talebtarik@ieee.org) is currently a professor at the School of Electrical Engineering, Aalto University. He has worked as senior researcher and 3GPP standards expert at NEC Europe Ltd. Prior to his work at NEC, until March 2009, he worked as an assistant professor at the Graduate School of Information Sciences, Tohoku University, Japan, in a lab fully funded by KDDI. He received his B.E. degree in information engineering with distinction, and his M.Sc. and Ph.D. degrees in information sciences from Tohoku University in 2001, 2003, and 2005, respectively. His research interests lie in the field of architectural enhancements to mobile core networks (particularly 3GPP's), mobile cloud networking, mobile multimedia streaming, and social media networking. He has also been directly engaged in the development and standardization of the Evolved Packet System. He is a member of the IEEE Communications Society Standardization Program Development Board and serves as Steering Committee Chair of the IEEE Conference on Standards for Communications and Networking. He has received many awards for his many contributions to the area of mobile networking.

Bin Li [S'12, M'14] received his Ph.D. degree from the School of Electronics and Information Engineering, Xi'an Jiaotong University, in 2014. From 2012 to 2013, he was a visiting student in the University of Louisville, Kentucky. He is currently an assistant professor at Northwest Polytechnical University. His research interests include network coding, channel measurement, the Internet of Things, and array signal processing.

Heng Qin [S'14] received his B.S. degree from Northwestern Polytechnical University in 2014, where he is currently an M.Sc. student. His research interests include wireless channel modeling, communications signal processing, and massive MIMO.

Zhimeng Zhong received his B.Sc., M.Sc., and Ph.D. degrees from Xi'an Jiaotong University in 2002, 2005, and 2008, respectively, all in electronic engineering. From 2009 to 2013, he was an algorithm engineer with Huawei Technologies Ltd., Xi'an. After working with the Research Institute of Aerospace Radio Technology in 2014, he rejoined Huawei Technologies Ltd., Shanghai. His current research interests include digital wireless communications, wireless channel measurement and modeling, and multiple-input multiple-output systems.

Xiaomei Zhang received her B.S. and M.S. degrees from Xi'an Jiaotong University in 2005 and 2008, respectively. Since 2008, she has been an algorithm engineer of Huawei Technologies Ltd.. Her research interests include wireless channel measurement and modeling and MIMO systems.

Another avenue of interest is the channel characterization for the millimeter-wave (mmWave) capabilities at the frequencies such as 28 and 38 GHz. The mmWave communications are expected to provide multi-gigabit rates to further enhance the backhaul capacity.